OBSTETRICS

Placental transcriptional and histologic subtypes of normotensive fetal growth restriction are comparable to preeclampsia

Isaac Gibbs[1]; Katherine Leavey, PhD[1]; Samantha J. Benton, PhD; David Grynspan, MD; Shannon A. Bainbridge, PhD; Brian J. Cox, PhD

BACKGROUND: Infants born small for gestational age because of pathologic placenta-mediated fetal growth restriction can be difficult to distinguish from those who are constitutionally small. Additionally, even among fetal growth–restricted pregnancies with evident placental disease, considerable heterogeneity in clinical outcomes and long-term consequences has been observed. Gene expression studies of fetal growth–restricted placentas also have limited consistency in their findings, which is likely due to the presence of different molecular subtypes of disease. In our previous study on preeclampsia, another heterogeneous placenta-centric disorder of pregnancy, we found that, by clustering placentas based only on their gene expression profiles, multiple subtypes of preeclampsia, including several with co-occurring suspected fetal growth restriction, could be identified.

OBJECTIVE: The purpose of this study was to discover placental subtypes of normotensive small-for-gestational-age pregnancies with suspected fetal growth restriction through the use of unsupervised clustering of placental gene expression data and to investigate their relationships with hypertensive suspected fetal growth–restricted placental subtypes.

STUDY DESIGN: A new dataset of 20 placentas from normotensive small-for-gestational-age pregnancies (birthweight <10th percentile for gestational age and sex) with suspected fetal growth restriction (ultrasound features of placental insufficiency) underwent genome-wide messenger RNA expression assessment and blinded detailed histopathologic evaluation. These samples were then combined with a subset of samples from our previously published preeclampsia cohort (n=77) to form an aggregate fetal growth-focused cohort (n=97) of placentas from normotensive small-for-gestational-age, hypertensive (preeclampsia and chronic hypertensive) small-for-gestational-age, and normotensive average-for-gestational-age pregnancies. Gene expression data were subjected to unsupervised clustering, and clinical and histopathologic features were correlated to the identified sample clusters.

RESULTS: Clustering of the aggregate dataset revealed 3 transcriptional subtypes of placentas from normotensive small-for-gestational-age/suspected fetal growth–restricted pregnancies, with differential enrichment of clinical and histopathologic findings. The first subtype exhibited either no placental disease or mild maternal vascular malperfusion lesions, and, co-clustered with the healthy average-for-gestational-age control subjects; the second subtype showed more severe evidence of hypoxic damage and lesions of maternal vascular malperfusion, and the third subtype demonstrated an immune/inflammatory response and histologic features of a maternal-fetal interface disturbance. Furthermore, all 3 of these normotensive small-for-gestational-age subtypes co-clustered with a group of placentas from hypertensive small-for-gestational-age pregnancies with more severe clinical outcomes, but very comparable transcriptional and histologic placental profiles.

CONCLUSION: Overall, this study provides evidence for at least 2 pathologic placental causes of normotensive small-for-gestational-age, likely representing true fetal growth restriction. These subtypes also show considerable similarity in gene expression and histopathology to our previously identified "canonical" and "immunologic" preeclampsia placental subtypes. Furthermore, we discovered a subtype of normotensive small-for-gestational-age (with suspected fetal growth restriction) with minimal placental disease that may represent both constitutionally small infants and mild fetal growth restriction, although these cannot be distinguished with the currently available data. Future work that focuses on the identification of etiology-driven biomarkers and therapeutic interventions for each subtype of fetal growth restriction is warranted.

Key words: clustering, fetal growth restriction, gene expression, histopathology, hypertension, microarray, placenta, preeclampsia, small-for-gestational-age

Fetal growth restriction (FGR) is the failure of a fetus to achieve its genetic growth potential in utero. FGR is associated with a significantly increased risk of stillbirth, preterm delivery, and neonatal death;[1–3] the potential consequences for infants who survive are extensive.[4–7] Although fetal size varies naturally across the population, pathologic growth restriction is suspected clinically when a fetus or infant falls below a critical size threshold and is identified as being small-for-gestational-age (SGA), either antenatally by ultrasound scan or by birthweight at delivery, respectively. Although this enriches for true cases of FGR, it also captures many fetuses and neonates who are constitutionally small and are at low risk for adverse outcomes.[8] The ability to identify FGR fetuses accurately within the SGA population would improve clinical care by targeting resources to fetuses and infants truly at risk of adverse perinatal outcome and reducing unnecessary interventions in pregnancies with constitutionally small fetuses.[9–11]

Although maternal,[12,13] fetal,[14,15] and environmental[16–18] factors can contribute to disrupted fetal growth,

EDITORS' CHOICE

Cite this article as: Gibbs I, Leavey K, Benton SJ, et al. Placental transcriptional and histologic subtypes of normotensive fetal growth restriction are comparable to preeclampsia. Am J Obstet Gynecol 2019;220:110.e1-21.

0002-9378/free

https://doi.org/10.1016/j.ajog.2018.10.003

Click Supplemental Materials under article title in Contents at ajog.org

AJOG at a Glance

Why was this study conducted?

The study was conducted to identify subtypes of placentas from pregnancies with suspected fetal growth restriction and to assess differences in their transcriptional, histologic, and clinical profiles.

Key Findings

On the basis of gene expression differences, we identified placental subtypes of suspected fetal growth restriction that demonstrated distinct histologic features. All 3 subtypes were associated with both normotensive and hypertensive mothers, which suggests significant maternal influence on the hypertensive response to placental dysfunction. Placental subtypes could be separated with the use of expression values for only 3 genes (LIMCH1, TAP1, and FLT1) by quantitative polymerase chain reaction.

What does this add to what is known?

Clustering of transcriptional data from suspected fetal growth restricted placentas, along with detailed clinical and histologic phenotyping, has never been done before. Subtypes of normotensive small-for-gestational-age were discovered and characterized, which opened up many avenues for future investigation.

placental dysfunction is considered the dominant cause of FGR.[19–23] Molecular analyses of FGR placentas have revealed aberrations in hypoxia, inflammation, endocrine signaling, and metabolism pathways,[24–28] and various histologic assessments have identified signs of maternal vascular malperfusion,[29] fetal thromboocclusive lesions,[29] and evidence of placental rejection by the maternal immune system,[30,31] the latter of which is associated with miscarriage and high rates of disease recurrence.[32,33] This broad range of contributors to placental dysfunction suggests that FGR is a complex and heterogeneous disease and challenges our ability to understand the disease cause.[11,34–36]

Large-scale gene expression analysis with the use of microarrays or RNA-sequencing is an excellent method for discovering novel molecular subtypes of human disease and has been used widely to great success in the field of oncology.[37] By applying unsupervised clustering methods and correlative analysis to gene expression data, statistically distinct groups of patients with different clinical phenotypes can be identified.[38,39] Furthermore, cohesive sets of differentially expressed genes often indicate specific cellular, developmental, or signaling pathways as possible causes or contributors to the disease.[40] In the reproductive biology field, gene expression studies have been conducted on placentas from pregnancies that were complicated by FGR and/or preeclampsia.[24,25,41–44] Preeclampsia is another heterogeneous placenta-centric disorder of pregnancy that has been suggested to share several pathologic features with FGR and, frequently, these diseases co-occur.[45–48] Curiously, comparisons across all studies focused on FGR or preeclampsia have found that only a small number of gene expression changes are consistently identified, which leads to calls for increased sample sizes to improve power.[49,50] However, we hypothesize that the main issues in FGR research are not small sample sizes, but rather the employment of an experimental design that considers only 2 possible states (disease vs healthy) and the inclusion of constitutionally small fetuses and neonates in the disease category. We propose that the use of unsupervised clustering to identify subtypes of suspected FGR cases will correct for both of these issues.

In our previous work, we sought to explicitly test if in preeclampsia, as in oncology, multiple molecular diseases can be responsible for the same clinical phenotype. We found that, by using unsupervised clustering techniques, novel placental subtypes of this hypertensive disorder could be identified successfully.[38,51] Specifically, within a large cohort of 330 placentas that represented a wide range of preeclampsia clinical presentations and co-occurring complications (SGA, chronic hypertension [CH], and preterm labor), clustering revealed 5 patient groups based solely on placental gene expression, which included 4 subtypes of preeclampsia samples within clusters 1, 2, 3, and 5 (cluster 4 was composed almost exclusively of preterm control placentas with chorioamnionitis).[38] Using a combined transcriptional,[38] clinical,[38] epigenetic,[52] and histopathologic[53] approach, we have further described each of these distinct preeclampsia placental subtypes: cluster 1 preeclampsia samples demonstrated molecular similarity to healthy term control placentas and very little placental disease, which suggests that this may be a predominately "maternal" preeclampsia subtype that is driven by preexisting, subclinical, maternal cardiovascular disease; cluster 2 preeclampsia was termed "canonical", with overwhelming evidence of maternal vascular malperfusion and placental hypoxia; cluster 3 contained a less prevalent "immunologic" subtype of preeclampsia that was marked by signs of heightened immune response at the maternal-fetal interface, similar to an allograft rejection;[30,31] and, finally, a subtype of preeclamptic placentas with chromosomal abnormalities, but no other strong clinical, epigenetic, or histologic association, was discovered in cluster 5. Notably, patients with both maternal hypertension (preeclampsia or CH) and SGA split across all 4 of these clusters.

Motivated by these findings, in the current study, we apply a similar molecular profiling approach to determine whether placental subtypes of normotensive FGR also exist and span the spectrum of placental dysfunction described for preeclampsia. To accomplish this, we assembled a combined fetal growth-focused microarray dataset that consisted of placentas from normotensive and hypertensive SGA pregnancies with suspected FGR, in addition to healthy control placentas, and applied unsupervised clustering methods. It is

postulated that this analysis will (1) appropriately separate constitutionally small normotensive SGA cases from the normotensive SGA cases with placenta-mediated growth restriction (ie, true FGR), (2) identify distinct subtypes of FGR with divergent underlying placental disease, and (3) reveal relationships to subtypes of placental disease previously discovered in hypertensive pregnancies. If successful, the identification of truly growth-restricted fetuses/infants, in addition to the placental disease underlying the cause of the growth restriction, would allow for targeted management of pregnancies at the highest risk of short- and long-term consequences.

Methods

The purpose of this study was to investigate the diversity of placental phenotypes related to FGR in both normotensive and hypertensive mothers. This was accomplished as a retrospective case-control study by selecting patient samples from a biobank that met the criteria for SGA (<10th percentile) with a reference in their clinical chart to suspected FGR based on ultrasound measurements of placental or uterine blood flow. These samples were then combined with healthy control and SGA placentas from our previous preeclampsia-focused cohort.[38] Analysis was performed with the use of a data-directed method whereby samples are grouped based on placental gene expression alone without reference to any clinical findings (unsupervised clustering). These results were then correlated to clinical and histopathologic data to validate the molecular groupings of the patient samples.

Placenta sample collection

Matched snap-frozen and formalin-fixed, paraffin-embedded placental tissue from 20 normotensive pregnancies with SGA infants (N-SGA) were purchased from the Research Centre for Women's and Infants' Health BioBank (Toronto, Canada). SGA was defined as birthweight <10th percentile for gestational age (GA) and sex, based on a Canadian growth reference.[54] All samples came from singleton pregnancies with live births that occurred after 34 weeks of gestation and were flagged by the BioBank as suspected FGR based on either signs of placental insufficiency by ultrasound scanning performed at Mount Sinai Hospital or a note in the clinical file from a previous care center. These pregnancies will be referred to throughout the manuscript as N-SGA with suspected FGR. This is done to avoid bias in our assessment of the molecular and clinical data, because there may be constitutionally small neonates within the suspected group. Placentas that were associated with maternal smoking, diabetes mellitus (preexisting or gestational), sickle cell anemia, morbid obesity (body mass index $\geq$40 kg/m^2), and/or clear evidence of a fetal cause of reduced growth (eg, genetic anomaly) were excluded.

Microarray gene expression assessment

Similar to our previous preeclampsia profiling study,[38] placental sampling for messenger RNA assessment was performed by the BioBank, such that 1 biopsy sample was collected, midway between the umbilical cord insertion and disc periphery, from each quadrant in the placenta. All 4 biopsy samples from each placenta were immediately rinsed in phosphate-buffered saline solution, pooled, snap-frozen in liquid nitrogen, and crushed into a powder. Messenger RNA was extracted from the 20 N-SGA snap-frozen tissues with the use of Trizol and RNAeasy spin columns, as well as from 4 average-for-gestational-age (AGA) control placentas previously purchased and used in our preeclampsia study[38] to serve as technical replicates. Extracted messenger RNA for all 24 placentas was hybridized against Human Gene 1.0 ST Array chips (Affymetrix, Santa Clara, CA) by the Princess Margaret Genomics Centre (Toronto, Canada). The generated microarray dataset for the 20 new N-SGA samples is available on the Gene Expression Omnibus, under the accession number GSE100415.

Dataset aggregation, unsupervised clustering, and principal component analysis

To investigate relationships between normotensive and hypertensive SGA pregnancies with suspected FGR, relevant samples from our previous preeclampsia cohort with available matched microarray, histologic, and clinical information[38,53] were also included in the current analysis (n=77). These consisted of samples classified as preeclampsia and SGA (preeclampsia-SGA; n=37), CH and SGA (CH-SGA; n=14), or normotensive term AGA control samples (N-AGA; n=26). Most of these SGA infants were also flagged as suspected FGR, but, in some cases, very little antenatal data were available. At the time of original sample collection, preeclampsia was defined as the onset of systolic pressure $\geq$140 mm Hg and/or diastolic pressure $\geq$90 mm Hg after the 20th week of gestation, accompanied by proteinuria (>300 mg protein/day or $\geq$2+ by dipstick).[55] CH was defined as systolic pressure $\geq$140 mm Hg and/or sustained diastolic pressure $\geq$90 mm Hg before the 20th week of gestation, and SGA was defined as earlier. Given our previous identification of very similar placental gene expression and histologic profiles between cases of preeclampsia and CH,[38,53] these 2 groups were analyzed together frequently as a single hypertensive group (H-SGA; n=51). Microarray data for these original 77 samples are available under the Gene Expression Omnibus accession number GSE75010.

Using the oligo library,[56] raw probe level microarray data from both cohorts (the N-SGA cohort; n=24, including the 4 technical replicate control samples) and the previous preeclampsia cohort (n=77) were read into R 3.2.1 software and normalized with the use of the robust multiarray average expression measure.[57] Empirical Bayes batch correction and conversion of probe level annotations to human gene symbols were performed with the use of the *virtualArray* package.[58] The 4 control technical replicates were removed from the combined SGA dataset after confirmation that they aligned with the original samples on a *t*-distributed stochastic neighbor embedding plot[59] (which robustly preserves nearest neighbor relationships) after batch correction (Supplementary Figure). Genes with a mean expression value in the bottom

quartile across all placentas were considered to be indistinguishable from background noise and therefore were filtered out.

To identify potential subtypes of placental disease in pregnancies with suspected FGR, unsupervised mixture-model–based clustering (*mclust* package; https://cran.r-project.org/web/packages/mclust/vignettes/mclust.html)[60] was applied to the top quartile of most variable genes in the 97 placenta samples, as previously described.[38] The optimal number of patient clusters was selected automatically based on the Bayesian Information Criterion and visualized by principal component analysis, a method that allows us to visualize the spread and relationships between clusters, using the *plot3d* function. The stability of the clusters was investigated with the use of the *clusterboot* function,[61] with 1000 bootstrap resamples of the data and the "noisemclustCBI" cluster method. This function quantifies the likelihood that a cluster is discovered in repeated experiments.

Quantitative polymerase chain reaction (qPCR) validation

In our previous preeclampsia study, we developed a panel of 3 genes (TAP1, LIMCH1, and FSTL3) that could separate placentas into clusters 1–4 based on the expression values that were obtained with the use of standard qPCR methods.[38] However, since then, we have discovered that 1 of these genes (FSTL3) is an unreliable marker and appears to be influenced easily by minor differences in experimental design. Using machine-learning algorithms and the original preeclampsia cohort qPCR data, as previously described,[38] FLT1 was found to be a good replacement for FSTL3. In the current study, validation of this second qPCR panel was performed with 17 of 20 new N-SGA samples with sufficient tissue available after microarray analysis. Briefly, extracted messenger RNA was converted into complementary DNA with ThermoFisher's High-Capacity RNA-to-cDNA Kit (Thermo Fisher Scientific Inc, Waltham, MA) and human TaqMan primer/probes sets were obtained from Applied Biosystems (Foster City, CA) for TAP1 (Hs00388675_m1), LIMCH1 (Hs00405524_m1), and FLT1 (Hs01052961_m1). The qPCR reaction was performed by a Life Technologies QuantStudio 7 Flex Real-Time PCR System with default TaqMan cycling conditions, and samples were run in duplicate and averaged for analysis. The mean cycle threshold values that were obtained for each of the 3 genes (TAP1, LIMCH1, and FLT1) were compared within a given placenta and used to classify each of the 17 samples into a molecular cluster. This method of taking the ratio of gene expression values within a sample abrogates the need for a common reference gene between samples.

Pathway enrichment analysis

To determine the likely underlying biologic mechanisms responsible for the gene expression clustering that was observed, pathway enrichment analysis was performed that compared each of the N-SGA subtypes to the cluster 1 N-AGA control samples, which consistently have demonstrated the healthiest placental profiles. Further, pathway enrichment analysis was also performed between co-clustering N-SGA and H-SGA placentas within each of the identified clusters and between the cluster 2 and cluster 3 N-SGA samples. This was done with the use of a modified version of the *sigpathway* algorithm,[62–65] all possible genes (n=14,038), and the Hallmark and GO gene sets (version 6.1) downloaded from the Molecular Signatures Database (Broad Institute, Inc., Cambridge, MA).[66,67] These Hallmark and GO gene sets consist of genes with a preestablished commonality and are organized in a hierarchic manner (eg, genes involved in DNA initiation, DNA priming, and DNA unwinding are also categorized as involved in DNA replication). Hallmark gene sets represent stable and well-defined biologic activities (n=50 total), while the large number of GO gene sets (n=5917 total) are each composed of genes that are involved in a particular biologic process, cellular component, or molecular function.[66] Pathways with 10–1000 members were assessed with 1000 permutations. Gene sets were considered significantly differentially expressed when they achieved both a competitive probability of $<.05$ and a NEk q-value $<.05$. A full description of the algorithm is in the Supplementary Material: Methods.

Histopathologic analysis

Matched formalin-fixed, paraffin-embedded tissue and historic placenta disease reports obtained from the Research Centre for Women's and Infants' Health BioBank for the 20 N-SGA samples underwent detailed histopathologic evaluation, as previously described.[53] Briefly, tissue biopsy samples were collected from each quadrant of the placenta, midway between the umbilical cord insertion, and the disc periphery. Tissue was fixed in formalin, embedded in paraffin wax, sectioned (5 μm), and stained with hematoxylin and eosin according to standard laboratory protocol.[68] Digital images of each slide were examined by an experienced placental pathologist who was blinded to molecular results and clinical information (apart from GA at delivery). Placentas were assessed for pathologic features with a standardized data collection form;[53] definitions and severity criteria were derived from practice and consensus guidelines.[69–73] Lesions were scored on a scale of 0–1 (absence/presence), 0–2, or 0–3 (assessing degree of severity) where appropriate. Individual lesions were also grouped into 1 of 8 broad disease categories of biologic significance and category sums were calculated.

Clinical characteristics

Similar to our preeclampsia cohort study,[38] >50 clinical variables were analyzed as either a continuous numeric or a categoric feature. Placental weight percentiles were computed,[74] and measured uterine and umbilical artery pulsatility indices (PIs) were compared with reference ranges for GA.[75,76] Estimated fetal weight was also converted to a percentile for GA[54,77] and placental efficiency was estimated based on the birthweight:placental weight ratio.[78] Birthweight was calculated as a percentile by 2 methods: a population-based Canadian reference[54] with the use of

GA and sex only, and a customized percentile calculator[79,80] based on maternal height, weight, ethnicity, and parity in addition to GA and sex. In an attempt to confirm a diagnosis of FGR in suspected patients, all available ultrasound data that may have indicated placental insufficiency was assessed and noted, which included uterine artery notching, uterine artery PI >95th percentile for GA, umbilical artery PI >95th percentile for GA, abnormal umbilical artery blood flow (absent end-diastolic velocity, reverse end-diastolic velocity, and/or increased resistance), in addition to other indications, such as nonconcordant placental grading (eg, placental grade III at 35 weeks gestation), placental lakes, echogenic cysts, wedge infarcts, signs of a "wobbly" placenta, and/or abnormal placental size, shape, or texture.

Statistics

Assessment of phenotype distributions and clinical and histopathologic differences across the clusters and subtypes was performed with Kruskal-Wallis rank-sum tests, Fisher's exact tests, and Mann-Whitney-Wilcoxon tests, as appropriate. Pearson correlations were used to assess the relationships between the birthweight percentiles that were obtained from the population reference and the customized reference.

Ethics approval

Ethics approval for this study was granted from the Research Ethics Boards of Mount Sinai Hospital (#13-0211-E), the Ottawa Health Science Network (#2011623-01H), and the University of Toronto (#29435). All women provided written informed consent for the collection of biologic specimens and medical information.

Results

Unsupervised clustering and qPCR validation

After successful batch correction (Supplementary Figure) and removal of the technical replicates and lowly expressed genes across all placentas, the final combined fetal growth–focused dataset for analysis contained 97 samples and 14,038 genes. Unsupervised clustering of these 97 placentas based solely on their gene expression profiles identified 3 clusters of placentas (Figure 1, A). Of these, clusters 1 and 2 were highly stable (ie, an average Jaccard similarity >0.8 across clusterings of bootstrap resamples of the data), although cluster 3 was somewhat less stable (0.67 average Jaccard similarity between the bootstrapped reclusters; Figure 1, B), likely, at least in part, because of its smaller size. Cluster 1 contained the majority (92%) of the N-AGA control samples, along with one-half (10/20) of the N-SGA samples and some (14%) of the H-SGA placentas (Figure 1, C; Table 1). The remaining one-half of the N-SGA samples split between clusters 2 and 3, co-clustering with the majority of the H-SGA samples. This implies the existence of 3 molecular N-SGA subtypes in this cohort, 1 in each of clusters 1–3.

Principal component analysis discovered 2 components (principal components 1 and 2) that alone accounted for 27% of the variability in the data. Visualization of the transcriptional data along these components revealed that, within clusters 2 and 3, the N-SGA samples appear to integrate well with the rest of the cluster (Figure 1, A and C). However, within cluster 1, the majority of the N-SGA placentas formed a distinct group, along with the cluster 1 H-SGA samples, at the border of cluster 2, separate from the healthy control samples (Figure 1, A and C). Notably, samples belonging to cluster 1 were delivered at significantly later GAs than those belonging to clusters 2 and 3 ($P<.01$; Figure 1, D). Visualization of the data along other components revealed differences in fetal sex (principal component 3) or similar patterns to those already identified (principal components 4–8) and are therefore not shown.

For the 77 placentas that were obtained from our previous preeclampsia cohort,[38] cluster inclusion was compared between our previous analysis and the current investigation. Samples that previously belonged to clusters 1–3 retained highly similar cluster memberships, although those with previous cluster 5 inclusion predominately collapsed into cluster 2 (Figure 2, A). Additionally, 17 of the 20 new N-SGA placentas (those with available tissue) were assessed for cluster inclusion with the use of our identified 3-gene qPCR panel (Figure 2, B). Of these, 11 (65%) showed complete agreement between the microarray and qPCR cluster assignment, although 2 samples (12%) were on the border of the correct and an incorrect cluster by qPCR and 4 samples (24%) were classified falsely (Figure 2, C). In both the preeclampsia cohort and the N-SGA placentas, samples with cluster discordance between the 2 molecular analyses (microarray and microarray or microarray and qPCR) plotted on the border of the 2 possible clusters by principal component analysis (Figure 2, A and C), which suggests transcriptional contributions from both groups.

Pathway enrichment analysis between and within clusters

To characterize the underlying molecular differences that drove the formation of the 3 N-SGA placental subtypes, we performed pathway enrichment analysis. Given that almost all of the healthy control (N-AGA) samples in this study were found together in cluster 1, we considered these placentas to be representative of "normal" gene expression and initially compared the N-SGA samples in clusters 1, 2, and 3 with these cluster 1 control samples. Unsurprisingly, pathway enrichment analysis found only a small number of significantly differentially expressed gene sets ($P<.05$ and $q<.05$) between the cluster 1 N-SGA and control samples (n=1 Hallmark sets; n=55 GO sets; Supplementary Table 1). The few enriched pathways in the N-SGA samples were associated with carbohydrate metabolism and hypoxia, while the under-expressed gene sets generally were involved in immune response.

In contrast, many significant differences were observed in the cluster 2 N-SGA (n=6 Hallmark sets; n=266 GO sets) and cluster 3 N-SGA (n=17 Hallmark sets; n=464 GO sets) samples when assessed against the cluster 1 control samples and compared with each

FIGURE 1
Principal component analysis visualization of the stability and composition of the 3 patient clusters identified by unsupervised clustering of the placental gene expression

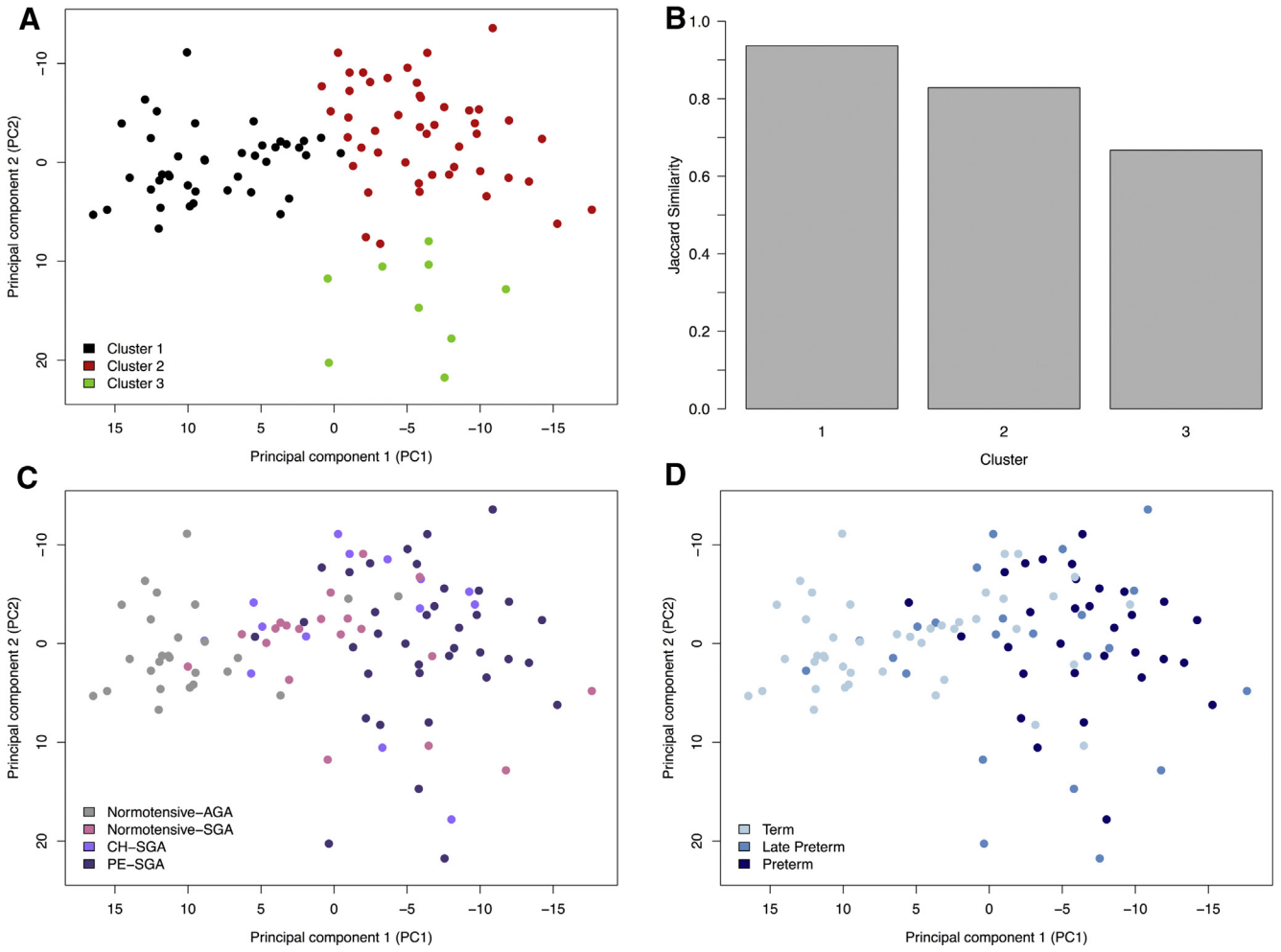

A, Cluster 1 (*black*) separated from cluster 2 (*red*) and cluster 3 (*green*) across principal component 1, while cluster 2 and 3 samples showed differences along principal component 2. **B**, A bar plot of the average Jaccard similarities from the *clusterboot* analysis revealed that all 3 clusters were relatively stable, although cluster 3 was somewhat less so (<0.8 Jaccard similarity between the bootstrapped reclusters). **C**, Normotensive average-for-gestational-age control subjects (*grey*) were found to populate the exterior edge of cluster 1. The portion of cluster 1 closest to cluster 2, and both clusters 2 and 3, contained a mix of normotensive small-for-gestational-age samples (*pink*), chronic hypertensive small-for-gestational-age samples (*light purple*), and preeclamptic small-for-gestational-age samples (*dark purple*). **D**, Cluster 1 placentas were delivered at notably later gestational ages than the placentas that belonged to clusters 2 and 3. Term deliveries (>37 weeks gestation) are shown in *light blue*; late preterm deliveries (34—37 weeks gestation) are in *medium blue*, and preterm deliveries (<34 weeks gestation) are in *dark blue*.

AGA, average-for-gestational-age; *CH*, chronic hypertensive; *PC1*, principal component 1; *PC2*, principal component 2; *SGA*, small-for-gestational-age.

Gibbs et al. Molecular placental subtypes of normotensive FGR. Am J Obstet Gynecol 2019.

other (n=11 Hallmark sets; n=207 GO sets; Supplementary Tables 2, 3, and 4). Cluster 2 N-SGA placentas exhibited an upregulation of genes associated with metabolism, hormone activity and secretion, feeding behavior, oxygen binding, and hypoxia, and a depletion of genes involved in immune response, cell proliferation, and muscle relaxation (Supplementary Tables 2 and 4). Cluster 3 N-SGA samples demonstrated a significant enrichment in immune, inflammatory, and cytokine activity genes and some hypoxia, coagulation, and apoptosis pathways and a down-regulation of protein metabolism and secretion pathways (Supplementary Tables 3 and 4).

Furthermore, to determine whether there were any biologically meaningful transcriptional differences between the normotensive and hypertensive placentas within a given cluster, the N-SGA and H-SGA samples in each cluster were also compared by pathway enrichment analysis. Within clusters 1 and 2, almost no gene sets were identified as

TABLE 1
Cluster composition by neonatal size and maternal hypertension status

Phenotype	Cluster, n (%)		
	1	2	3
Normotensive average-for-gestational-age (n=26)	24 (92)	2 (8)	0 (0)
Normotensive small-for-gestational-age (n=20)	10 (50)	7 (35)	3 (15)
Chronic hypertensive small-for-gestational-age (n=14)	5 (36)	7 (50)	2 (14)
Preeclamptic small-for-gestational-age (n=37)	2 (5)	31 (84)	4 (11)
Hypertensive small-for-gestational-age (n=51)[a]	7 (14)	38 (75)	6 (12)
Total (n=97)	41 (42)	47 (48)	9 (9)

[a] Includes both preeclamptic and chronic hypertensive small-for-gestational-age samples.
Gibbs et al. Molecular placental subtypes of normotensive FGR. Am J Obstet Gynecol 2019.

significantly different between the normotensive and hypertensive SGA samples (Supplementary Tables 1 and 2). However, in cluster 3, a few significant pathways were discovered (n=0 Hallmark sets; n=34 GO sets); the N-SGA placentas exhibited an overexpression of gene sets that were involved in lipid metabolism and epigenetic functions, such as demethylation and histone acetylation (Supplementary Table 3).

Histopathologic analysis of the transcriptional clusters

We next investigated whether the 3 N-SGA subtypes differed in their histopathologic profiles compared with the control samples, each other, and their co-clustering H-SGA placentas. Overall, the cluster 1 N-SGA samples demonstrated minimal histopathology, with almost identical cumulative disease scores to the cluster 1 N-AGA control samples (1.80 vs 1.83; P=.94; Table 2). Ten placentas in cluster 1 (7 N-AGA and 3 N-SGA) had no observed histologic lesions whatsoever. However, in the remaining placentas, the types of lesions that were observed between the cluster 1 N-AGA and cluster 1 N-SGA groups were different. The N-AGA control samples showed some signs of delayed villous maturity, intervillous thrombi, villitis of unknown etiology, and/or meconium histiocytes, that covered a range of different categories of biologic significance. The N-SGA placentas showed mild severity lesions of maternal vascular malperfusion (MVM), such as syncytial knots and accelerated villous maturity (MVM sum 1.70 in the N-SGA placentas vs 0.50 in the N-AGA control samples; P=.01). The H-SGA samples that belonged to this cluster also showed lesions of MVM almost exclusively, although with a higher degree of severity compared with the normotensive placentas (3.29 vs 1.70; P=.05).

Although both the N-SGA and the H-SGA samples in cluster 2 exhibited some thrombosis and intervillous thrombi lesions, the majority of the observed histopathologic evidence in this cluster were lesions of MVM (Table 2). Further, the cluster 2 H-SGA placentas revealed the highest MVM score sums in the entire cohort (4.87), followed by the cluster 2 N-SGA samples (3.43; P<.01 across the cohort; P=.15 to each other). In contrast, cluster 3 samples uniquely demonstrated increased frequency and severity of histopathologic lesions that were consistent with a maternal-fetal interface disturbance (P=.01), such as massive perivillous fibrin deposition (P<.01), and evidence of chronic inflammation (P=.05; Table 2). Additionally, both the N-SGA and H-SGA placentas in this cluster showed signs of MVM lesions, although the disease was again more severe in the H-SGA placentas (3.33 vs 1.00; P=.05).

Clinical characteristics of the clusters

The clinical characteristics of the 3 N-SGA subtypes were compared with each other, the cluster 1 control samples, and the H-SGA samples (Table 3; Supplementary Table 5). Across the entire cohort, the population and customized birthweight percentiles were highly correlated (Pearson correlation coefficient=0.97; P<.01). In general, the cluster 1 N-SGA samples appeared the healthiest of the N-SGA subtypes, with the least reduced birthweights (P=.29 [population reference] and P=.01 [customized method] across the N-SGA subtypes), the latest GAs at delivery (P=.14; Figure 1, D), and the most efficient placentas (P=.19). Two cluster 1 N-SGA infants that had been classified as <5th percentile for birthweight with the use of the population reference were assessed at the 10th and 15th percentiles based on the customized method. Of the 9 of 10 pregnancies with available ultrasound data in this N-SGA subtype, 78% (7/9) demonstrated at least 1 ultrasound indication of placental insufficiency, although none of these were associated with abnormal uterine artery blood flow to the placenta (eg, high uterine artery PI or notching). These 2 pregnancies without signs of placental insufficiency on ultrasound scan were not the ones that resulted in infants with conflicting birthweight percentiles.

In contrast, the cluster 2 and 3 N-SGA patients exhibited more severe clinical outcomes (Table 3; Supplementary Table 5). These infants were delivered slightly earlier (P=.14 across the N-SGA subtypes; Figure 1, D) and were associated with more nonreassuring uterine and umbilical Doppler findings (P=.05−.09). Uterine artery notching was most commonly observed in cluster 2 N-SGA (P=.07 across the N-SGA subtypes), although cluster 3 N-SGA patients were associated with peripherally inserted umbilical cords (P=.07) and were most likely to have experienced a previous SGA pregnancy (P=.21) and/or stillbirth (P=.17). All N-SGA subjects with placentas in clusters 2 and 3 and available ultrasound data (9/10) demonstrated clear evidence of placental insufficiency during pregnancy. Interestingly, 1 cluster 2 N-SGA infant who had been classified at the 10th percentile for birthweight based on the population

FIGURE 2
Principal component analysis visualization of the cluster inclusion validations

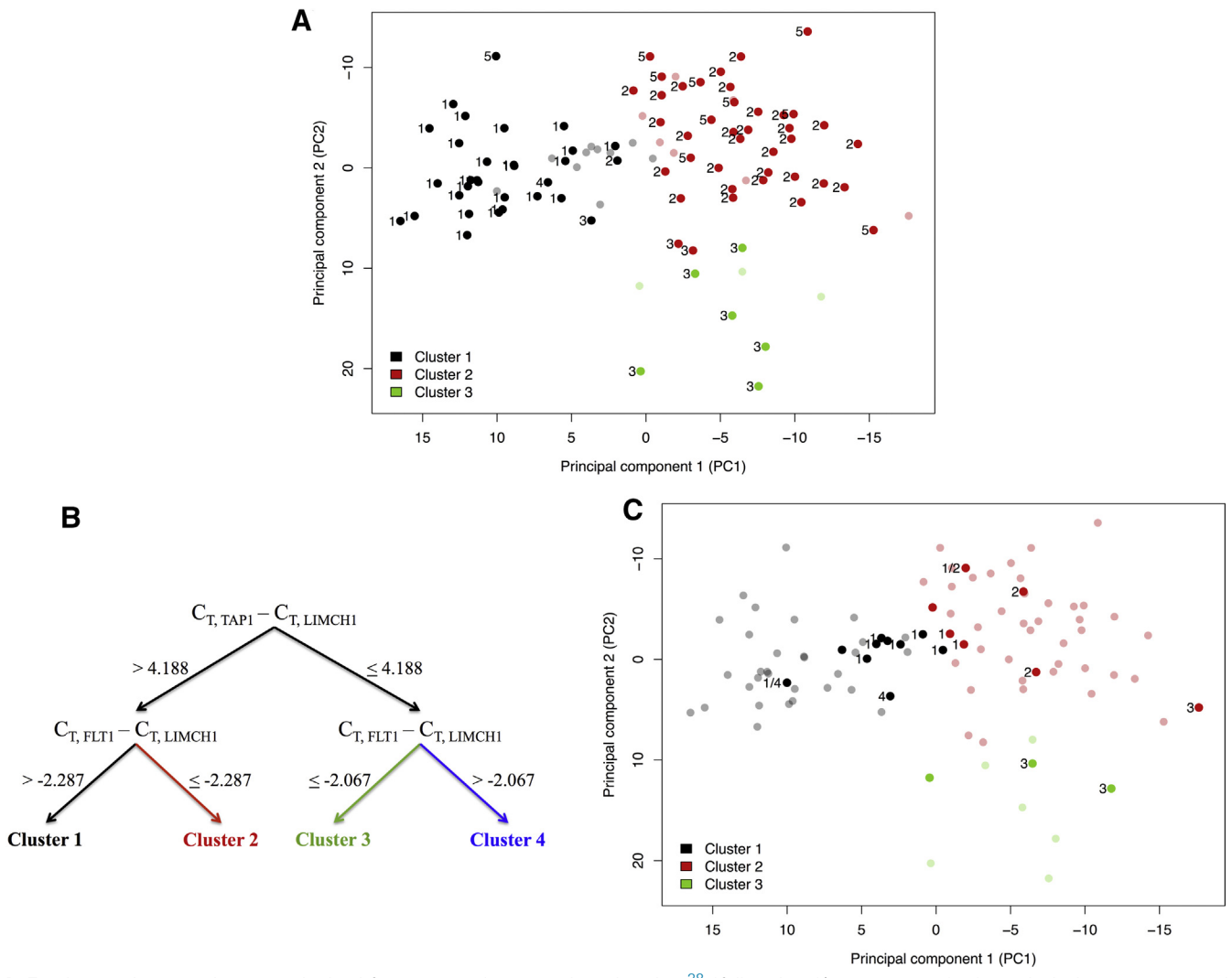

A, For the 77 placentas that were obtained from our previous preeclamptic cohort[38] (*fully colored/not transparent*), cluster inclusion was compared between our previous analysis (numbers 1—5 represent clusters 1—5) and the current assessment (*colors black, red, and green represent clusters 1-3, respectively*). Samples previously belonging to clusters 1—3 retained highly similar cluster memberships, while those with previous cluster 5 inclusion predominately collapsed into cluster 2. The 20 new normotensive small-for-gestational-age samples are shown in *semitransparent colors*. **B,** Simple quantitative polymerase chain reaction differences in the mean cycle threshold values that represent FLT1, LIMCH1, and TAP1 gene expression were found to be capable of distinguishing between clusters 1 (*black*), 2 (*red*), 3 (*green*), and 4 (*blue*) in our previous preeclamptic cohort.[38] Clusters 1—3 each contained varying proportions of patients with preeclampsia, as described earlier, although cluster 4 consisted of preterm control placentas with chorioamnionitis. The immune-associated clusters 3 and 4 demonstrated more similar expression of TAP1 and LIMCH1 than the nonimmune clusters 1 and 2, whereas the preeclampsia-enriched clusters 2 and 3 revealed elevated FLT1 expression compared with LIMCH1. **C**, Of the 20 new normotensive small-for-gestational-age placentas (*fully colored/not transparent*), 17 placentas had remaining available tissue and were utilized to validate the 3-gene quantitative polymerase chain reaction panel in **B**. Of these, 11 samples (65%) showed complete agreement between the microarray (*colors black, red, and green represent clusters 1—3*) and quantitative polymerase chain reaction (numbers 1—4 represent clusters 1—4) cluster assignment, although 2 samples (12%) were on the border of the correct and an incorrect cluster by quantitative polymerase chain reaction (shown with a "/") and 4 samples (24%) were classified falsely. The 77 samples from the preeclamptic-cohort are shown in *semitransparent colors*. In both **A** and **C**, samples with cluster discordance between the 2 molecular analyses (colors and numbers) plotted on the border of the 2 possible clusters by principal component analysis, which suggests transcriptional contributions from both groups.

C_T, cycle threshold.

Gibbs et al. Molecular placental subtypes of normotensive FGR. Am J Obstet Gynecol 2019.

TABLE 2
Histopathologic comparison of the molecular subtypes by fetal growth and maternal hypertensive status

Histopathologic lesion[a]	Cluster[b] 1 Normotensive average-for-gestational-age (n=24)	1 Normotensive small-for-gestational-age (n=10)	1 Hypertensive small-for-gestational-age (n=7)	2 Normotensive small-for-gestational-age (n=7)	2 Hypertensive small-for-gestational-age (n=38)	3 Normotensive small-for-gestational-age (n=3)	3 Hypertensive small-for-gestational-age (n=6)	*P* value[c]
Maternal vascular malperfusion								
Distal villous hypoplasia (n=46)	0 (0)	0.30 (0.48)	1.14 (0.69)	0.57 (0.79)	1.29 (0.77)	0 (0)	0.50 (0.55)	<.01
Placental infarctions (n=40)	0.12 (0.34)	0.30 (0.48)	0.29 (0.49)	0.57 (0.79)	1.03 (0.79)	0 (0)	0.33 (0.52)	< .01
Accelerated villous maturity (n=51)	0.04 (0.20)	0.40 (0.52)	0.71 (0.49)	0.71 (0.49)	0.84 (0.37)	0.33 (0.58)	0.50 (0.55)	< .01
Syncytial knots (n=59)	0.21 (0.41)	0.50 (0.53)	1.00 (0.58)	0.71 (0.49)	1.18 (0.65)	0.33 (0.58)	0.83 (0.75)	< .01
Focal perivillous fibrin (n=23)	0.12 (0.34)	0.10 (0.32)	0 (0)	0.29 (0.49)	0.34 (0.48)	0.33 (0.58)	0.83 (0.98)	.10
Villous agglutination (n=3)	0 (0)	0 (0)	0 (0)	0.43 (0.79)	0.03 (0.16)	0 (0)	0 (0)	.01
Decidual vasculopathy (n=11)	0 (0)	0.10 (0.32)	0.14 (0.38)	0.14 (0.38)	0.16 (0.37)	0 (0)	0.33 (0.52)	.32
Category sum (n=75)	0.50 (0.66)	1.70 (1.42)	3.29 (1.38)	3.43 (2.51)	4.87 (2.00)	1.00 (1.00)	3.33 (1.21)	< .01
Implantation site abnormalities								
Microscopic accreta (n=1)	0 (0)	0 (0)	0 (0)	0.14 (0.38)	0 (0)	0 (0)	0 (0)	.05
Increased basement membrane fibrin (n=0)	0 (0)	0 (0)	0 (0)	0 (0)	0 (0)	0 (0)	0 (0)	—
Category sum (n=1)	0 (0)	0 (0)	0 (0)	0.14 (0.38)	0 (0)	0 (0)	0 (0)	.05
Histologic chorioamnionitis								
Maternal inflammation (n=0)	0 (0)	0 (0)	0 (0)	0 (0)	0 (0)	0 (0)	0 (0)	—
Fetal inflammation (n=0)	0 (0)	0 (0)	0 (0)	0 (0)	0 (0)	0 (0)	0 (0)	—
Vessel thrombosis (n=0)	0 (0)	0 (0)	0 (0)	0 (0)	0 (0)	0 (0)	0 (0)	—
Category sum (n=0)	0 (0)	0 (0)	0 (0)	0 (0)	0 (0)	0 (0)	0 (0)	—
Placenta villous maldevelopment								
Chorangiosis (n=2)	0.08 (0.28)	0 (0)	0 (0)	0 (0)	0 (0)	0 (0)	0 (0)	.43
Chorangioma (n=2)	0 (0)	0 (0)	0 (0)	0 (0)	0.03 (0.16)	0.33 (0.58)	0 (0)	.02
Delayed villous maturity (n=12)	0.29 (0.46)	0 (0)	0 (0)	0 (0)	0.05 (0.23)	0 (0)	0.50 (0.55)	< .01
Category sum (n=15)	0.38 (0.58)	0 (0)	0 (0)	0 (0)	0.08 (0.27)	0.33 (0.58)	0.50 (0.55)	.01

Gibbs et al. Molecular placental subtypes of normotensive FGR. Am J Obstet Gynecol 2019.

(continued)

TABLE 2
Histopathologic comparison of the molecular subtypes by fetal growth and maternal hypertensive status *(continued)*

Histopathologic lesion[a]	Cluster[b] 1 Normotensive average-for-gestational-age (n=24)	1 Normotensive small-for-gestational-age (n=10)	1 Hypertensive small-for-gestational-age (n=7)	2 Normotensive small-for-gestational-age (n=7)	2 Hypertensive small-for-gestational-age (n=38)	3 Normotensive small-for-gestational-age (n=3)	3 Hypertensive small-for-gestational-age (n=6)	*P* value[c]
Fetal vascular malperfusion								
Avascular fibrotic villi (n=2)	0 (0)	0 (0)	0 (0)	0 (0)	0.03 (0.16)	0 (0)	0.17 (0.41)	.30
Thrombosis (n=7)	0.04 (0.20)	0 (0)	0 (0)	0.14 (0.38)	0.11 (0.31)	0 (0)	0.17 (0.41)	.71
Intramural fibrin deposition (n=0)	0 (0)	0 (0)	0 (0)	0 (0)	0 (0)	0 (0)	0 (0)	—
Category sum (n=9)	0.04 (0.20)	0 (0)	0 (0)	0.14 (0.38)	0.13 (0.34)	0 (0)	0.33 (0.52)	.27
Chronic uteroplacental separation								
Chorionic hemosiderosis (n=2)	0.04 (0.20)	0 (0)	0 (0)	0.14 (0.38)	0 (0)	0 (0)	0 (0)	.34
Retroplacental hematoma (n=5)	0.04 (0.20)	0 (0)	0 (0)	0 (0)	0.08 (0.27)	0 (0)	0.17 (0.41)	.73
Laminar necrosis (n=0)	0 (0)	0 (0)	0 (0)	0 (0)	0 (0)	0 (0)	0 (0)	—
Category sum (n=7)	0.08 (0.28)	0 (0)	0 (0)	0.14 (0.38)	0.08 (0.27)	0 (0)	0.17 (0.41)	.83
Maternal-fetal interface disturbance								
Massive perivillous fibrin deposition (n=5)	0 (0)	0 (0)	0 (0)	0 (0)	0.03 (0.16)	0.33 (0.58)	0.50 (0.55)	< .01
Maternal floor infarction pattern (n=1)	0 (0)	0 (0)	0 (0)	0 (0)	0 (0)	0 (0)	0.17 (0.41)	.02
Intervillous thrombi (n=19)	0.25 (0.44)	0 (0)	0.14 (0.38)	0.29 (0.49)	0.16 (0.37)	0.67 (0.58)	0.50 (0.84)	.20
Category sum (n=21)	0.25 (0.44)	0 (0)	0.14 (0.38)	0.29 (0.49)	0.18 (0.46)	1 (1)	1.17 (1.17)	.01
Chronic inflammation								
Infectious villitis (n=0)	0 (0)	0 (0)	0 (0)	0 (0)	0 (0)	0 (0)	0 (0)	—
Villitis of unknown etiology (n=8)	0.21 (0.59)	0 (0)	0.29 (0.76)	0 (0)	0.05 (0.23)	0.67 (1.15)	0.33 (0.82)	.40
Chronic intervillositis (n=3)	0 (0)	0 (0)	0 (0)	0 (0)	0.03 (0.16)	0.67 (1.15)	0.17 (0.41)	.03
Chronic deciduitis (n=10)	0.08 (0.28)	0.10 (0.32)	0.14 (0.38)	0.14 (0.38)	0.05 (0.23)	0.33 (0.58)	0.33 (0.52)	.38
Category sum (n=16)	0.29 (0.81)	0.10 (0.32)	0.43 (0.79)	0.14 (0.38)	0.13 (0.41)	1.67 (2.08)	0.83 (1.17)	.05

Gibbs et al. Molecular placental subtypes of normotensive FGR. Am J Obstet Gynecol 2019.

(continued)

TABLE 2
Histopathologic comparison of the molecular subtypes by fetal growth and maternal hypertensive status *(continued)*

Histopathologic lesion[a]	Cluster[b]							
	1			2		3		
	Normotensive average-for-gestational-age (n=24)	Normotensive small-for-gestational-age (n=10)	Hypertensive small-for-gestational-age (n=7)	Normotensive small-for-gestational-age (n=7)	Hypertensive small-for-gestational-age (n=38)	Normotensive small-for-gestational-age (n=3)	Hypertensive small-for-gestational-age (n=6)	*P* value[c]
Additional features								
Meconium histiocytes/macrophages within membranes (n=9)	0.29 (0.46)	0 (0)	0 (0)	0 (0)	0.03 (0.16)	0 (0)	0.17 (0.41)	.01
Meconium-induced myonecrosis (n=1)	0 (0)	0 (0)	0 (0)	0 (0)	0.03 (0.16)	0 (0)	0 (0)	.96
Cumulative pathology score: overall sum (n=85)	1.83 (1.61)	1.80 (1.40)	3.86 (0.9)	4.29 (2.36)	5.53 (2.19)	4.00 (1.00)	6.50 (1.64)	< .01

[a] Of 95 possible samples; N indicates the number of samples with a non-zero score. The 2 normotensive small-for-gestational-age placentas that were found in cluster 2 were not included in this Table because they belong to neither a small-for-gestational-age subgroup of interest or the healthy cluster 1 normotensive average-for-gestational-age comparison group. However, they showed minimal histopathologic evidence (cumulative scores of 1 and 2) that indicated that their inclusion in cluster 2 is likely due to an anomaly in the microarray data and/or preprocessing, because they do not appear to form a biologically significant subtype; [b] Data are given as mean (standard deviation); [c] Based on nonparametric Kruskal-Wallis rank sum tests.

Gibbs et al. Molecular placental subtypes of normotensive FGR. Am J Obstet Gynecol 2019.

reference was assessed at the 2nd percentile with the use of the customized method.

Last, a number of clinical attributes were found to be significantly different among all 3 N-SGA subtypes compared with their hypertensive counterparts. Across the cohort, the N-SGA group demonstrated lower mean uterine artery PIs ($P<.01$), lower mean umbilical artery PIs ($P<.01$), fewer cesarean section deliveries ($P<.01$), later GAs at delivery ($P<.01$), higher Apgar scores ($P<.05$), and lower rates of infant transfers to the neonatal intensive care unit ($P=.06$) compared with the H-SGA group (Table 3; Supplementary Table 5). Furthermore, none of the N-SGA women had experienced a previous hypertensive pregnancy, in contrast to 58% of the possible (primiparous and multiparous) H-SGA patients ($P<.01$).

Comment

Principal findings

In this study, we assessed the placental gene expression of a fetal growth-focused cohort using unsupervised clustering methods and identified 3 molecular subtypes of placentas from N-SGA pregnancies with suspected FGR. Samples that belonged to the first N-SGA subtype (10/20 N-SGA patients, 50%) demonstrated an intermediate gene expression pattern between the healthy control samples of cluster 1 (N-AGA samples) and the cluster 2 N-SGA samples, with either no evidence of placental histopathologic disease or lesions of mild MVM. Cluster 2 N-SGA placentas (7/20 N-SGA patients, 35%) were characterized by poor uterine artery blood flow and substantial MVM lesions (eg, distal villous hypoplasia, accelerated villous maturity, and syncytial knots), while the rarer cluster 3 N-SGA placentas (3/20 N-SGA patients, 15%) were associated with maternal-fetal interface disturbance lesions (eg, massive perivillous fibrin deposition and intervillous thrombi) and features of chronic inflammation (eg, villitis of unknown etiology and chronic intervillositis). These 3 N-SGA subgroups could be separated with the use of our developed TAP1, LIMCH1, and FLT1

TABLE 3
Important clinical characteristics of the molecular subtypes, by fetal growth and maternal hypertensive status

Clinical attribute	Cluster 1: Normotensive average-for-gestational-age (n=24)	Cluster 1: Normotensive small-for-gestational-age (n=10)	Cluster 1: Hypertensive small-for-gestational-age (n=7)	Cluster 2: Normotensive small-for-gestational-age (n=7)	Cluster 2: Hypertensive small-for-gestational-age (n=38)	Cluster 3: Normotensive small-for-gestational-age (n=3)	Cluster 3: Hypertensive small-for-gestational-age (n=6)	*P* value[a]
Maternal demographics								
Maternal height, cm[b]	163 (7)	161 (9)	160 (7)	167 (10)	163 (7)	160 (7)	159 (5)	.63
Previous miscarriage, % (n/N)	29 (7/24)	30 (3/10)	29 (2/7)	29 (2/7)	29 (11/38)	67 (2/3)	33 (2/6)	.93
Previous hypertensive pregnancy, % (n/N)	7 (1/14)	0 (0/7)	50 (2/4)	0 (0/2)	64 (7/11)	0 (0/2)	50 (2/4)	.01
Previous small-for-gestational-age pregnancy, % (n/N)	7 (1/14)	43 (3/7)	75 (3/4)	0 (0/2)	18 (2/11)	100 (2/2)	50 (2/4)	.01
Previous stillbirth, % (n/N)	0 (0/14)	0 (0/7)	25 (1/4)	0 (0/3)	9 (1/11)	50 (1/2)	25 (1/4)	.09
Ultrasound characteristics[b]								
Last noted estimated fetal weight[c]	50 (16)	3 (2)	14 (18)	5 (8)	1 (1)	3 (4)	1 (1)	< .01
Mean uterine artery pulsatility index[d]	—	0.88 (0.11)	1.91 (0.23)	1.25 (0.46)	1.81 (0.43)	1.23 (0.36)	1.62 (0.57)	<.01
Mean umbilical artery pulsatility index[d]	0.98 (0.08)	1.10 (0.15)	1.76 (0.65)	1.36 (0.35)	1.67 (0.40)	1.28 (0.07)	1.44 (0.32)	<.01
Assessed ultrasound evidence of placental insufficiency, % (n/N)								
Uterine artery notching[d]	0 (0/1)	0 (0/4)	67 (2/3)	80 (4/5)	90 (19/21)	33 (1/3)	60 (3/5)	<.01
Uterine artery pulsatility index above the 95th percentile for gestational age[d]	0 (0/1)	0 (0/5)	100 (3/3)	80 (4/5)	100 (21/21)	67 (2/3)	80 (4/5)	<.01
Umbilical artery pulsatility index above the 95th percentile for gestational age[d]	0 (0/6)	75 (6/8)	100 (5/5)	83 (5/6)	83 (25/30)	100 (3/3)	100 (6/6)	<.01
Noted abnormal umbilical artery blood flow[d,e]	0 (0/6)	29 (2/7)	60 (3/5)	67 (4/6)	84 (27/32)	67 (2/3)	50 (3/6)	<.01
Other signs of placental insufficiency[d,f]	33 (1/3)	56 (5/9)	60 (3/5)	60 (3/5)	37 (10/27)	67 (2/3)	40 (2/5)	.83
At least 1 of the above	17 (1/6)	78 (7/9)	83 (5/6)	100 (6/6)	94 (31/33)	100 (3/3)	100 (6/6)	<.01
At least 2 of the above	0 (0/6)	44 (4/9)	83 (5/6)	100 (6/6)	82 (27/33)	100 (3/3)	67 (4/6)	<.01
Hypertensive disease in pregnancy, % (n/N)								
Chronic hypertension	0 (0/24)	0 (0/10)	71 (5/7)	0 (0/7)	37 (14/38)	0 (0/3)	50 (3/6)	<.01
Preeclampsia diagnosis	0 (0/24)	0 (0/10)	29 (2/7)	0 (0/7)	82 (31/38)	0 (0/3)	67 (4/6)	<.01

Gibbs et al. Molecular placental subtypes of normotensive FGR. Am J Obstet Gynecol 2019.

(continued)

TABLE 3
Important clinical characteristics of the molecular subtypes, by fetal growth and maternal hypertensive status *(continued)*

Clinical attribute	Cluster 1			Cluster 2		Cluster 3		*P* value[a]
	Normotensive average-for-gestational-age (n=24)	Normotensive small-for-gestational-age (n=10)	Hypertensive small-for-gestational-age (n=7)	Normotensive small-for-gestational-age (n=7)	Hypertensive small-for-gestational-age (n=38)	Normotensive small-for-gestational-age (n=3)	Hypertensive small-for-gestational-age (n=6)	
Delivery								
Gestational age at delivery, wk[b]	39 (1)	38 (1)	35 (4)	36 (1)	32 (3)	37 (1)	33 (4)	<.01
Delivery <34 weeks, % (n/N)	0 (0/24)	0 (0/10)	29 (2/7)	0 (0/7)	68 (26/38)	0 (0/3)	50 (3/6)	<.01
Delivery <37 weeks, % (n/N)	8 (2/24)	20 (2/10)	71 (5/7)	43 (3/7)	89 (34/38)	67 (2/3)	100 (6/6)	<.01
Fetal demographics								
Male fetus, % (n/N)	58 (14/24)	40 (4/10)	43 (3/7)	43 (3/7)	55 (21/38)	33 (1/3)	17 (1/6)	.61
Birthweight (percentile)[b]	50 (23)	3 (3)	3 (2)	3 (4)	3 (4)	1 (1)	3 (5)	< .01
Birthweight <5th percentile for gestational age and sex, % (n/N)	0 (0/24)	60 (6/10)	29 (2/7)	83 (5/6)	55 (21/38)	100 (3/3)	83 (5/6)	<.01
Customized birthweight (percentile)[b]	52 (28)	5 (4)	2 (3)	1 (1)	1 (2)	1 (1)	0 (1)	<.01
Neonatal intensive care unit transfer, % (n/N)	0 (0/24)	10 (1/10)	43 (3/7)	29 (2/7)	42 (16/38)	33 (1/3)	67 (4/6)	<.01
Placental and umbilical cord characteristics[b]								
Placental weight (percentile)	48 (40)	12 (22)	8 (18)	4 (8)	5 (17)	18 (31)	2 (5)	< .01
Placental efficiency, ratio	5.34 (0.67)	5.49 (0.80)	5.45 (1.04)	4.60 (0.75)	4.49 (1.01)	4.70 (2.15)	4.70 (1.11)	.01

NOTE: For data given as mean (standard deviation), the data were only noted and used if values were available for at least 2 samples in the subtype group: for data given as percentage of the group (subsample/total number of samples), all available data were used within these 7 subtype groups; however, information was missing for some samples for some characteristics.

[a] Based on nonparametric Kruskal-Wallis rank sum tests or Fisher's exact tests, as appropriate; [b] Data given as mean (standard deviation); [c] Within the last 4 weeks of pregnancy; [d] Ultrasound measurements across all of pregnancy were included; [e] Such as absent end-diastolic velocity, reverse end-diastolic velocity, and/or increased resistance; [f] Descriptions of nonconcordant placental grading, placental lakes, echogenic cysts, wedge infarcts, a "wobbly" placenta, and/or abnormal placental size, shape, or texture.

Gibbs et al. Molecular placental subtypes of normotensive FGR. Am J Obstet Gynecol 2019.

qPCR panel with a reasonable degree of accuracy. Furthermore, each of these N-SGA subtypes coclustered with placentas from hypertensive SGA pregnancies (H-SGA). Within each cluster, the molecular and histologic profiles of the normotensive and hypertensive samples were comparable, which confirmed the considerable placental resemblance between N-SGA and H-SGA cases,[36,45] but the clinical characteristics of the hypertensive patients, which included significantly more restricted uterine artery blood flow and earlier deliveries to avoid worsening maternal and fetal outcomes, were, unsurprisingly, more severe than the normotensive patients. This indicates that hypertension may be less a function of etiologic differences in the placenta and more representative of the diversity of maternal physiologic adaptations to the placental dysfunction.

Results in context

The concept that FGR is a multifactorial, heterogeneous disease has been around for decades.[29,34,81,82] Despite this, previous attempts to characterize the underlying pathophysiologic causes of this disorder generally have focused on the binary comparison of a small infant/fetus group to a healthy control group of infants/fetuses. By using an unsupervised approach, 3 distinct molecular subtypes of placentas from N-SGA pregnancies have been identified. The healthiest N-SGA placentas fell into subtype 1 (cluster 1), which indicated that this group may contain both constitutionally small infants (likely those where the customized growth calculation placed them above the 10th percentile and/or those with no signs of placental insufficiency on ultrasound scan) and infants who were mildly growth restricted in utero because of placental insufficiency. It is also possible that some of these patients could be associated with an unknown fetal cause of growth restriction,[14,15] although these 3 possibilities are not readily distinguishable with the currently available information. In contrast, the second and third placental N-SGA subtypes identified in clusters 2 and 3, respectively, had more severe clinical features, such as lower newborn infant weights and earlier deliveries. These samples also showed clear signs of placental disease, both molecularly and histologically, and exhibited consistent evidence of placental insufficiency by ultrasound scans. Therefore, we believe that clusters 2 and 3 identify 2 subtypes of true pathologic growth restriction: "hypoxic" FGR and "immunologic" FGR.

An additional finding of interest was the co-clustering of placentas from normotensive and hypertensive SGA pregnancies in each cluster, which suggested similar underlying placental causes in these groups, regardless of maternal hypertensive state. Although somewhat in contrast to the identification of little to no significant molecular differences between the normotensive and hypertensive SGA placentas in each cluster, hypertensive samples did exhibit moderately more severe lesions of MVM than their normotensive counterparts ($P=.05$ in clusters 1 and 3; $P=.15$ in cluster 2). This mild discrepancy could be attributed to the timing of placental sampling (molecular alterations associated with the MVM disease may no longer be visible[83,84]), minor sampling differences (the snap-frozen and formalin-fixed, paraffin-embedded tissues are not the exact same biopsy samples), and differences in statistical thresholds (histologic results are reported as nominal probability values, while the molecular pathways are corrected for multiple-hypothesis testing). Given the general similarities in gene expression and histopathologic evidence in the co-clustering SGA groups, we suspect that variation in the maternal response to a given placental profile is primarily responsible for the hypertensive or normotensive state.[47] These observations emphasize the importance of considering both maternal and fetal contributions to the disease process. Unfortunately, matched maternal samples were not available for these patients but will be essential in subsequent studies to address this theory directly. Last, because we used a retrospective study design, we cannot determine whether there is a relative increased risk of hypertension because of placental disease.

Clinical implications

Accurately distinguishing between placental FGR and constitutionally small fetuses would represent a significant improvement for clinical care and allow for resources to be targeted appropriately to high-risk fetuses. Here, we reported 3 clinically relevant groups of SGA fetuses, each with distinct molecular, histologic, and clinical phenotypes. Importantly, the healthiest of the SGA pregnancies, likely containing some constitutionally small fetuses (cluster 1), grouped away from the 2 clusters where the SGA fetuses likely represent true FGR (clusters 2 and 3). Investigating placental biomarkers and clinical assessments, such as uterine and umbilical artery Doppler tests, from the perspective of these 3 clusters may allow for improved detection and diagnostic performance. For example, decreased maternal plasma placental growth factor is suggested to reflect placental dysfunction antenatally; however, results between FGR studies vary, probably because of the inclusion of constitutionally small fetuses with healthy placentas in the FGR group. We postulate that the FGR pregnancies with placentas that belonged to clusters 2 and 3 would be identified accurately by placental growth factor.[85,86] Additionally, because the causes underlying cluster 2 and 3 are different, these 2 groups would likely benefit from different therapeutic approaches.[81,87] Furthermore, the immune-related cluster 3 histopathology is known to have much higher rates of recurrence in subsequent pregnancies[31,33,81,88–91] compared with the maternal malperfusion disease observed in cluster 2; therefore, postpartum counseling strategies for these distinct FGR patient groups may also differ. In fact, even with the limited obstetric history available to us in this cohort, it was noted that the cluster 3 N-FGR patients more commonly had experienced a previous SGA pregnancy and/or stillbirth. Our TAP1, LIMCH1, and FLT1 qPCR panel, which we have now validated, is able to predict FGR subtype membership fairly accurately and, when applied, may offer an easy modality to stratify patients after

delivery to identify those who are at highest risk for recurrence.

Research implications

From a research standpoint, the knowledge that placental subtypes of FGR exist and can be distinguished should impact study designs moving forward. Previously, we developed a small qPCR panel as a simple and convenient tool for the subclassification of placentas affected by preeclampsia. Importantly, this panel was validated successfully in the current study with new data that was independent of the samples that were used originally to define the classifier. This qPCR panel can discriminate placentas from cases of constitutionally small neonates from FGR that is affected by severe "hypoxic" and "immunologic" diseases. As such, this panel should be used for grouping samples into clusters before performing other large-scale studies (eg, metabolomics or maternal blood arrays) or for interrogating subtype-specific responses to treatment, without the need for a full genome analysis. In this way, underlying heterogeneity will not mask mechanistic changes or successful intervention or prediction results that are unique to 1 particular group and, hopefully, allow for significant progress to be made in this field.

Our findings of both variable maternal hypertensive states within a cluster and the diversity of placental histopathologic findings across the clusters warrant further investigation. The hypertensive state likely arises from either maternal sensitivity or robustness to placental dysfunction and stress factors that are released by the placenta. The immune response not only may be part of a spectrum of maladaptive immune rejection of the conceptus but also could be an exaggerated response to an infectious insult (viral) that leads to an autoimmune-like reaction against the placenta. These are important research questions for future investigation.

Strengths and limitations

The primary strength of this study was the application of unsupervised clustering to identify subtypes of disease and differentially expressed genes and gene sets. This approach was important for avoiding a subjective bias in patient classification. Another key strength was our comparison of hypertensive and normotensive suspected FGR pregnancies, where the similarities in placental gene expression and disease indicated a prominent role for the mother in the development of maternal symptoms. The histopathologic data were collected with the use of a standardized data collection form and blinding of the pathologist to the sample classification, which also helped to avoid biased findings that can arise by informing the observer. Last, we integrated detailed clinical information and histopathologic examination with the discovered sample clusters. The significant enrichment of specific clinical and histologic features to different subsets of samples provides high confidence that these groups are real and biologically meaningful.

This study does also have inherent limitations that we acknowledge. The 97 samples that were included in this cohort represent a substantial, but still relatively small, dataset, especially given the considerable complexity observed in placental diseases. A further increase in sample size and the inclusion of preterm (GA <34 weeks) N-SGA placentas may reveal additional subtypes of normotensive FGR. GA is significantly correlated with the severity of the disease; however, the relationship is not causal because the delivery is due to medical intervention. This is further supported by the observation that the normotensive cases do not show a significant GA-related distribution and co-cluster with the hypertensive cases, independent of GA differences. In addition, enriched gene sets between clusters 1 and 2 are not age-related. As such, although we do not believe that there is any indication that the results in the current study should be attributed to GA, interpretation of these data must always be done with this possible confounding effect in mind. Additionally, the almost exclusive assessment of samples annotated as SGA with suspected FGR likely limited the number of constitutionally small infants who were included in the current study. Using an unselected/prospectively collected SGA population may improve our capacity to distinguish easily and accurately constitutionally small from pathologically growth-restricted fetuses. Finally, 1 of the primary limitations is the unbalanced sample distribution, with substantially more SGA placentas that were associated with hypertensive pregnancies than normotensive pregnancies. As such, the samples from our previous preeclampsia cohort may be disproportionally responsible for the formation of the clusters. Therefore, the fact that no unique placental N-SGA subtypes were identified in the current analysis does not eliminate the possibility that they exist, simply that their potential discovery will require a further cohort expansion and a better balanced experimental design.

Conclusions

Overall, this study provides novel insight into at least 2 pathologic causes of normotensive FGR. Additionally, we discovered a high degree of similarity between normotensive and hypertensive FGR placentas, which indicates that it is feasible to maintain a maternal normotensive state until term despite a highly diseased placenta. As such, future research focused on each placental subtype of FGR, which includes an in-depth analysis of fetal vs maternal contributions to pregnancy outcome, may lead to the development of subtype-specific biomarkers and therapeutic targets capable of reducing the health burden of FGR. ■

Acknowledgments

The authors thank the donors and the Research Centre for Women's and Infants' Health (RCWIH) BioBank for the human samples used in this study and Jeremiah Gaudet (University of Ottawa) and Michal Leckie (University of Ottawa) for performing the RNA extractions.

References

1. Hoellen F, Beckmann A, Banz-Jansen C, Weichert J, Rody A, Bohlmann MK. Management of very early-onset fetal growth restriction: results from 92 consecutive cases. In Vivo 2016;30:123–31.

2. Story L, Sankaran S, Mullins E, et al. Survival of pregnancies with small for gestational age

detected before 24 weeks gestation. Eur J Obstet Gynecol Reprod Biol 2015;188:100–3.
3. Mendez-Figueroa H, Truong VTT, Pedroza C, Khan AM, Chauhan SP. Small-for-gestational-age infants among uncomplicated pregnancies at term: a secondary analysis of 9 Maternal-Fetal Medicine Units Network studies. Am J Obstet Gynecol 2016;215:628.e1–7.
4. Baschat AA, Viscardi RM, Hussey-Gardner B, Hashmi N, Harman C. Infant neurodevelopment following fetal growth restriction: relationship with antepartum surveillance parameters. Ultrasound Obstet Gynecol 2009;33:44–50.
5. Cohen E, Wong FY, Horne RS, Yiallourou SR. Intrauterine growth restriction: impact on cardiovascular development and function throughout infancy. Pediatr Res 2016;79:1–10.
6. Ronkainen E, Dunder T, Kaukola T, Marttila R, Hallman M. Intrauterine growth restriction predicts lower lung function at school age in children born very preterm. Arch Dis Child Fetal Neonatal Ed 2016;101:F412–7.
7. Ferguson AC. Prolonged impairment of cellular immunity in children with intrauterine growth retardation. J Pediatr 1978;93:52–6.
8. Royal College of Obstetricians and Gynaecologists. The Investigation and Management of the Small-for-Gestational-Age Fetus [Internet]. RCOG Green Top Guidelines. 2013. Available at: www.rcog.org.uk/clinical-guidance. Accessed June 10, 2018.
9. Zhang J, Merialdi M, Platt LD, Kramer MS. Defining normal and abnormal fetal growth: promises and challenges. Am J Obstet Gynecol 2010;202:522–8.
10. Soothill PW, Bobrow CS, Holmes R. Small for gestational age is not a diagnosis. Ultrasound Obstet Gynecol 1999;13:225–8.
11. Audette MC, Kingdom JC. Screening for fetal growth restriction and placental insufficiency. Semin Fetal Neonatal Med 2018;23:119–25.
12. Wang H, Hu YF, Hao JH, et al. Maternal zinc deficiency during pregnancy elevates the risks of fetal growth restriction: a population-based birth cohort study. Sci Rep 2015;5:11262.
13. Shin D, Song WO. Prepregnancy body mass index is an independent risk factor for gestational hypertension, gestational diabetes, preterm labor, and small- and large-for-gestational-age infants. J Matern Neonatal Med 2015;28:1679–86.
14. Wallenstein MB, Harper LM, Odibo AO, et al. Fetal congenital heart disease and intrauterine growth restriction: a retrospective cohort study. J Matern Fetal Neonatal Med 2012;25:662–5.
15. Khoury MJ, Erickson JD, Cordero JF, McCarthy BJ. Congenital malformations and intrauterine growth retardation: a population study. Pediatrics [Internet]. 1988;82(1):83—90. Available at: http://www.ncbi.nlm.nih.gov/pubmed/3380603. Accessed June 10, 2018.
16. Blatt K, Moore E, Chen A, Van Hook J, DeFranco EA. Association of reported trimester-specific smoking cessation with fetal growth restriction. Obstet Gynecol 2015;125:1452–9.
17. Virji SK. The relationship between alcohol consumption during pregnancy and infant birthweight: an epidemiologic study. Acta Obstet Gynecol Scand 1991;70:303–8.
18. Walker PG, ter Kuile FO, Garske T, Menendez C, Ghani AC. Estimated risk of placental infection and low birthweight attributable to Plasmodium falciparum malaria in Africa in 2010: a modelling study. Lancet Glob Heal 2014;2:e460–7.
19. Salafia CM, Minior VK, Pezzullo JC, Popek EJ, Rosenkrantz TS, Vintzileos AM. Intrauterine growth restriction in infants of less than thirty-two weeks' gestation: associated placental pathologic features. Am J Obstet Gynecol 1995;173:1049–57.
20. Kingdom JCP, Drewlo S. Is heparin a placental anticoagulant in high-risk pregnancies? Blood 2011;118:4780–8.
21. Triggianese P, Perricone C, Chimenti MS, De Carolis C, Perricone R. Innate Immune System at the Maternal-Fetal Interface: Mechanisms of disease and targets of therapy in pregnancy syndromes. Am J Reprod Immunol 2016;76:245–57.
22. Deter RL, Levytska K, Melamed N, Lee W, Kingdom JCP. Classifying neonatal growth outcomes: use of birthweight, placental evaluation and individualized growth assessment. J Matern Neonatal Med 2016;29:3939–49.
23. Burton GJ, Jauniaux E. Pathophysiology of placental-derived fetal growth restriction. Am J Obstet Gynecol 2018;218(suppl2):S745–61.
24. Sitras V, Paulssen R, Leirvik J, Vårtun A, Acharya G. Placental gene expression profile in intrauterine growth restriction due to placental insufficiency. Reprod Sci 2009;16:701–11.
25. Nishizawa H, Ota S, Suzuki M, et al. Comparative gene expression profiling of placentas from patients with severe pre-eclampsia and unexplained fetal growth restriction. Reprod Biol Endocrinol 2011;9:107.
26. McMinn J, Wei M, Schupf N, et al. Unbalanced placental expression of imprinted genes in human intrauterine growth restriction. Placenta 2006;27:540–9.
27. McCarthy C, Cotter FE, McElwaine S, et al. Altered gene expression patterns in intrauterine growth restriction: potential role of hypoxia. Am J Obstet Gynecol 2007;196:70.e1–6.
28. Struwe E, Berzl G, Schild R, et al. Microarray analysis of placental tissue in intrauterine growth restriction. Clin Endocrinol (Oxf) 2010;72:241–7.
29. Kovo M, Schreiber L, Ben-Haroush A, et al. The placental factor in early- and late-onset normotensive fetal growth restriction. Placenta 2013;34:320–4.
30. Romero R, Whitten A, Korzeniewski SJ, et al. Maternal floor infarction/massive perivillous fibrin deposition: a manifestation of maternal antifetal rejection? Am J Reprod Immunol 2013;70:285–98.
31. Faye-Petersen OM, Ernst LM. Maternal floor infarction and massive perivillous fibrin deposition. Surg Pathol Clin 2013;6:101–14.
32. Katzman PJ, Genest DR. Maternal floor infarction and massive perivillous fibrin deposition: histological definitions, association with intrauterine fetal growth restriction, and risk of recurrence. Pediatr Dev Pathol 2002;5:159–64.
33. Bane AL, Gillan JE. Massive perivillous fibrinoid causing recurrent placental failure. BJOG 2003;110:292–5.
34. Zimmer EZ, Divon MY. Sonographic diagnosis of IUGR-macrosomia. Clin Obstet Gynecol 1992;35:172–84.
35. Figueras F, Gratacos E. An integrated approach to fetal growth restriction. Best Pract Res Clin Obstet Gynaecol 2017;38:48–58.
36. Mifsud W, Sebire NJ. Placental pathology in early-onset and late-onset fetal growth restriction. Fetal Diagn Ther 2014;36:117–28.
37. Khan J, Wei JS, Ringnér M, et al. Classification and diagnostic prediction of cancers using gene expression profiling and artificial neural networks. Nat Med 2001;7:673–9.
38. Leavey K, Benton SJ, Grynspan D, Kingdom JC, Bainbridge SA, Cox BJ. Unsupervised placental gene expression profiling identifies clinically relevant subclasses of human preeclampsia. Hypertension 2016;68:137–47.
39. Lapointe J, Li C, Higgins JP, et al. Gene expression profiling identifies clinically relevant subtypes of prostate cancer. Proc Natl Acad Sci [Internet] 2004;101(3):811–6. Available at: http://www.pnas.org/cgi/doi/10.1073/pnas.0304146101. Accessed June 10, 2018.
40. Subramanian A, Tamayo P, Mootha VK, et al. Gene set enrichment analysis: a knowledge-based approach for interpreting genome-wide expression profiles. Proc Natl Acad Sci U S A 2005;102:15545–50.
41. Sitras V, Paulssen RH, Grønaas H, et al. Differential placental gene expression in severe preeclampsia. Placenta 2009;30:424–33.
42. Dunk CE, Roggensack AM, Cox B, et al. A distinct microvascular endothelial gene expression profile in severe IUGR placentas. Placenta 2012;33:285–93.
43. Várkonyi T, Nagy B, Füle T, et al. Microarray profiling reveals that placental transcriptomes of early-onset HELLP syndrome and preeclampsia are similar. Placenta 2011;32(suppl):S21–9.
44. Nishizawa H, Pryor-Koishi K, Kato T, Kowa H, Kurahashi H, Udagawa Y. Microarray analysis of differentially expressed fetal genes in placental tissue derived from early and late onset severe pre-eclampsia. Placenta 2007;28:487–97.
45. Babic I, Ferraro ZM, Garbedian K, et al. Intraplacental villous artery resistance indices and identification of placenta-mediated diseases. J Perinatol 2015;35:793–8.
46. Burton GJ, Yung HW, Cindrova-Davies T, Charnock-Jones DS. Placental endoplasmic reticulum stress and oxidative stress in the pathophysiology of unexplained intrauterine

growth restriction and early onset preeclampsia. Placenta 2009;30(suppl):43–8.
47. Stergiotou I, Bijnens B, Cruz-Lemini M, Figueras F, Gratacos E, Crispi F. Maternal subclinical vascular changes in fetal growth restriction with and without pre-eclampsia. Ultrasound Obstet Gynecol 2015;46:706–12.
48. Lyall F, Robson SC, Bulmer JN. Spiral artery remodeling and trophoblast invasion in preeclampsia and fetal growth restriction relationship to clinical outcome. Hypertension 2013;62:1046–54.
49. Kleinrouweler CE, van Uitert M, Moerland PD, Ris-Stalpers C, van der Post JAM, Afink GB. Differentially expressed genes in the pre-eclamptic placenta: a systematic review and meta-analysis. PLoS One 2013;8.
50. Tsai S, Hardison NE, James AH, et al. Transcriptional profiling of human placentas from pregnancies complicated by preeclampsia reveals disregulation of sialic acid acetylesterase and immune signalling pathways. Placenta 2011;32:175–82.
51. Leavey K, Bainbridge SA, Cox BJ. Large Scale Aggregate Microarray Analysis Reveals Three Distinct Molecular Subclasses of Human preeclampsia. PLoS One [Internet] 2015;10(2):e0116508. Available at: http://dx.plos.org/10.1371/journal.pone.0116508. Accessed June 10, 2018.
52. Leavey K, Wilson SL, Bainbridge SA, Robinson WP, Cox BJ. Epigenetic regulation of placental gene expression in transcriptional subtypes of preeclampsia. Clin Epigenetics 2018;10:28.
53. Benton SJ, Leavey K, Grynspan D, Cox BJ, Bainbridge SA. The clinical heterogeneity of preeclampsia is related to both placental gene expression and placental histopathology. Am J Obstet Gynecol 2018, https://doi.org/10.1016/j.ajog.2018.09.036. [Epub ahead of print].
54. Kramer MS, Platt RW, Wen SW, et al. A new and improved population-based Canadian reference for birth weight for gestational age. Pediatrics [Internet] 2001;108(2):e35-e35. Available at: http://pediatrics.aappublications.org/cgi/doi/10.1542/peds.108.2.e35. Accessed June 10, 2018.
55. Report of the National High Blood Pressure Education Program working group on high blood pressure in pregnancy. Am J Obstet Gynecol 2000;183(suppl):S1–22.
56. Carvalho BS, Irizarry RA. A framework for oligonucleotide microarray preprocessing. Bioinformatics 2010;26:2363–7.
57. Gautier L, Cope L, Bolstad BM, Irizarry RA. Affy: analysis of Affymetrix GeneChip data at the probe level. Bioinformatics 2004;20:307–15.
58. Heider A, Alt R. VirtualArray: a R/bioconductor package to merge raw data from different microarray platforms. BMC Bioinformatics [Internet]. 2013;14:75. Available at: http://www.pubmedcentral.nih.gov/articlerender.fcgi?artid=3599117&tool=pmcentrez&rendertype=abstract. Accessed June 10, 2018.
59. Van der Maaten L, Hinton GE. Visualizing high-dimensional data using t-SNE. J Mach Learn Res [Internet] 2008;9:2579–605. Available at: http://www.ncbi.nlm.nih.gov/entrez/query.fcgi?db=pubmed&cmd=Retrieve&dopt=AbstractPlus&list_uids=7911431479148734548related:VOiAgwMNy20J. Accessed June 10, 2018.
60. Scrucca L, Fop M, Murphy TB, Raftery AE. Mclust 5: clustering, classification and density estimation using Gaussian finite mixture models. R J 2016;8:289–317.
61. Hennig C. Cluster-wise assessment of cluster stability. Comput Stat Data Anal 2007;52:258–71.
62. Tian L, Greenberg SA, Kong SW, Altschuler J, Kohane IS, Park PJ. Discovering statistically significant pathways in expression profiling studies. Proc Natl Acad Sci U S A [Internet] 2005;102(38):13544–9. Available at: http://eutils.ncbi.nlm.nih.gov/entrez/eutils/elink.fcgi?dbfrom=pubmed&id=16174746&retmode=ref&cmd=prlinks%5Cnpapers3://publication/doi/10.1073/pnas.0506577102. Accessed June 10, 2018.
63. Ackermann M, Strimmer K. A general modular framework for gene set enrichment analysis. BMC Bioinformatics [Internet] 2009;10(1):47. Available at: http://www.biomedcentral.com/1471-2105/10/47%5Cnhttp://www.biomedcentral.com/content/pdf/1471-2105-10-47.pdf. Accessed June 10, 2018.
64. Goeman JJ, Bühlmann P. Analyzing gene expression data in terms of gene sets: methodological issues. Bioinformatics 2007;23:980–7.
65. Maciejewski H. Gene set analysis methods: statistical models and methodological differences. Brief Bioinform 2014;15:504–18.
66. Liberzon A, Subramanian A, Pinchback R, Thorvaldsdóttir H, Tamayo P, Mesirov JP. Molecular signatures database (MSigDB) 3.0. Bioinformatics 2011;27:1739–40.
67. Liberzon A, Birger C, Thorvaldsdóttir H, Ghandi M, Mesirov JP, Tamayo P. The molecular signatures database hallmark gene set collection. Cell Syst 2015;1:417–25.
68. Warrander LK, Batra G, Bernatavicius G, et al. Maternal perception of reduced fetal movements is associated with altered placental structure and function. PLoS One 2012;7.
69. Redline RW. Villitis of unknown etiology: noninfectious chronic villitis in the placenta. Hum Pathol 2007;38:1439–46.
70. Redline RW, Ariel I, Baergen RN, et al. Fetal vascular obstructive lesions: Nosology and reproducibility of placental reaction patterns. Pediatr Dev Pathol 2004;7(5):443–52.
71. Redline RW, Boyd T, Campbell V, Hyde S, Kaplan C, Khong TY, et al. Maternal vascular underperfusion: nosology and reproducibility of placental reaction patterns. Pediatr Dev Pathol [Internet]. 2004;7(3):237–49. Available at: http://www.ncbi.nlm.nih.gov/pubmed/15022063. Accessed June 10, 2018.
72. Redline RW, Faye-Petersen O, Heller D, Qureshi F, Savell V, Vogler C. Amniotic infection syndrome: nosology and reproducibility of placental reaction patterns. Pediatr Dev Pathol 2003;6:435–48.
73. Khong TY, Mooney EE, Ariel I, et al. Sampling and definitions of placental lesions Amsterdam placental workshop group consensus statement. Arch Pathol Lab Med 2016;140(7):698–713.
74. Connolloy AJ, Finkbeiner WE, Ursell PC, Davis RL. Autopsy pathology: a manual and atlas, 3rd ed. Philadelphia, PA: Elsevier Ltd; 2016.
75. Gómez O, Figueras F, Fernández S, et al. Reference ranges for uterine artery mean pulsatility index at 11-41 weeks of gestation. Ultrasound Obstet Gynecol 2008;32:128–32.
76. Acharya G, Wilsgaard T, Berntsen GK, Maltau JM, Kiserud T. Reference ranges for serial measurements of umbilical artery Doppler indices in the second half of pregnancy. Am J Obstet Gynecol 2005;192:937–44.
77. Hadlock FP, Harrist RB, Martinez-Poyer J. In utero analysis of fetal growth: a sonographic weight standard. Radiology [Internet]. 1991;181(1):129–33. Available at: http://pubs.rsna.org/doi/10.1148/radiology.181.1.1887021. Accessed June 10, 2018.
78. Hayward CE, Lean S, Sibley CP, et al. Placental adaptation: what can we learn from birthweight:placental weight ratio? Front Physiol 2016;7:28.
79. GROW (Gestation Related Optimal Weight: customised antenatal growth chart software. [Internet]. Gestation Network; Available at: http://www.gestation.net. Accessed June 10, 2018.
80. Gardosi J, Francis A, Turner S, Williams M. Customized growth charts: rationale, validation and clinical benefits. Am J Obstet Gynecol 2018;218(suppl):S609–18.
81. Kingdom JC, Audette MC, Hobson SR, Windrim RC, Morgen E. A placenta clinic approach to the diagnosis and management of fetal growth restriction. Am J Obstet Gynecol 2017;218(suppl2):S803–17.
82. Catov JM, Nohr EA, Olsen J, Ness RB. Chronic hypertension related to risk for preterm and term small for gestational age births. Obstet Gynecol 2008;112:290–6.
83. Fogarty NME, Ferguson-Smith AC, Burton GJ. Syncytial knots (Tenney-Parker changes) in the human placenta: evidence of loss of transcriptional activity and oxidative damage. Am J Pathol 2013;183:144–52.
84. Fitzgerald B, Levytska K, Kingdom J, Walker M, Baczyk D, Keating S. Villous trophoblast abnormalities in extremely preterm deliveries with elevated second trimester maternal serum hCG or inhibin-A. Placenta 2011;32:339–45.
85. Whitten AE, Romero R, Korzeniewski SJ, et al. Evidence of an imbalance of angiogenic/antiangiogenic factors in massive perivillous fibrin deposition (maternal floor infarction): a placental lesion associated with recurrent miscarriage and fetal death. Am J Obstet Gynecol 2013;208:310.e1–11.
86. Benton SJ, McCowan LM, Heazell AEP, et al. Placental growth factor as a marker of fetal growth restriction caused by placental dysfunction. Placenta 2016;42:1–8.
87. Chaiworapongsa T, Romero R, Korzeniewski SJ, et al. Pravastatin to prevent recurrent fetal death in massive perivillous fibrin

deposition of the placenta (MPFD). J Matern Neonatal Med 2016;29:855–62.

88. Contro E, DeSouza R, Bhide A. Chronic intervillositis of the placenta: A systematic review. Placenta [Internet]. Elsevier Ltd; 2010;31(12): 1106–10. Available at: https://doi.org/10.1016/j.placenta.2010.10.005. Accessed June 10, 2018.

89. Boyd TK, Redline RW. Chronic histiocytic intervillositis: a placental lesion associated with recurrent reproductive loss. Hum Pathol 2000;31:1389–96.

90. Chan JSY. Villitis of unknown etiology and massive chronic intervillositis. Surg Pathol Clin 2013;6:115–26.

91. Feeley L, Mooney EE. Villitis of unknown aetiology: correlation of recurrence with clinical outcome. J Obstet Gynaecol 2010;30: 476–9.

Author and article information

From the Departments of Physiology (Mr Gibbs, and Drs Leavey and Cox) and Obstetrics and Gynaecology (Dr Cox), University of Toronto, Toronto, Ontario, Canada; the Departments of Cellular and Molecular Medicine (Drs Benton and Bainbridge) and Pathology and Laboratory Medicine (Dr Grynspan), and the Interdisciplinary School of Health Sciences (Dr Bainbridge), University of Ottawa, Ottawa, Ontario, Canada.

[1]These authors contributed equally to this article.

Received June 20, 2018; revised Sept. 27, 2018; accepted Oct. 1, 2018.

Supported by the Canadian Institutes of Health Research Grant #128369 (S.A.B. and B.J.C.), an Undergraduate Summer Research Award from the University of Toronto (Department of Physiology; I.G.), an Ontario Graduate Scholarship (K.L.), and a Tier 2 Canada Research Chair in Placental Development and Maternal-Fetal Health (B.J.C.). S.J.B. is a Molly Towell Research Fellow.

The funding sources played no role in the study design, data collection and analysis, decision to publish, or preparation of the manuscript.

The authors report no conflict of interest.

Corresponding author: Brian J. Cox, PhD. b.cox@utoronto.ca

Supplementary Material

Methods

Pathway enrichment analysis was performed using a modified version of the *sigpathway* algorithm.[1] This algorithm tests 2 separate null hypotheses, which are denoted in the original work as Q1 and Q2, to determine whether gene sets are expressed differentially between the 2 groups that were under investigation. In our study, Q2, as implemented by Tian et al,[1] was tested for each gene set and a NEk q-value $<.05$ from this test was considered to constitute sufficient evidence of differential expression between sample groups. However, in many cases, we are interested not only in determining whether a given gene set is expressed differentially but also in evaluating whether this differential expression is causally responsible for the phenotypic differences that were observed. Q1, as proposed by Tian et al,[1] investigated this question by exploring whether a given gene set is expressed differentially relative to the global expression levels of all genes that were measured. In general, this method has been criticized for investigating a hypothesis that is discordant with the experimental design and thus is not interpretable mathematically.[2] As a result, we have chosen to replace this test with a heuristic, which was first proposed by Maciejewski,[2] that explores the same question as Q1 but does not form a formal statistical test. This heuristic is referred to as a competitive probability (P) and is used as a way to gather preliminary evidence about which of the differentially expressed gene sets (as identified by Q2) are most likely to explain the phenotypic differences that were observed. Formally, we let

$$P = \frac{1}{B}\sum_{i=1}^{B} I(|f(tmi)| > |f(t)|)$$

and G = the number of genes in the gene set of interest, where f is the mean function, t is the set of t-statistics for the gene set of interest, tmi for $i \in \{1,\ldots,B\}$ is a random draw of G t-statistics from the genes not in t, and B is the number of resamplings that were performed. This method returns an estimate of the probability that a random sample of G genes not in the gene set of interest realizes a mean t-statistic with a greater absolute value than the mean t-statistic of the genes in the gene set.

References

1. Tian L, Greenberg SA, Kong SW, Altschuler J, Kohane IS, Park PJ. Discovering statistically significant pathways in expression profiling studies. Proc Natl Acad Sci U S A 2005;102:13544–9.

2. Maciejewski H. Gene set analysis methods: statistical models and methodological differences. Brief Bioinform 2014;15:504–18.

Glossary

Appropriate-for-gestational-age (AGA): Neonatal birthweight >10th percentile for gestational age and sex.
Bayesian Information Criterion (BIC): Criterion for model selection that works by rewarding models that fit the data well while penalizing overly complicated models with a lot of parameters to avoid over-fitting the data. The model with the lowest BIC is considered to represent the optimal model.
Bootstrapping: Refers to any method that uses resampling with replacement.
Chronic hypertension: Systolic pressure ≥140 mm Hg and/or sustained diastolic pressure ≥90 mm Hg at <20 weeks gestation.
***clusterboot* function:** Function for measuring the stability of clusters. In general, a cluster is considered stable if it is robust to nonessential changes in the underlying data. In this case, we use this function to evaluate whether new identically sampled datasets would produce similar clusters.
Constitutionally small infant: Normally grown for maternal size and ethnicity and fetal sex.
Empirical Bayes batch correction: An algorithm for combining microarray expression data from multiple experiments by removing the effects of varying experimental conditions. The model assumes that the expression data arise from a linear combination of true signal, batch-specific effects, and random error. Model parameters are estimated with the use of a Bayesian approach, and batch effects are then removed to produce a final batch-corrected dataset.
Fetal growth restriction (FGR): The failure of a fetus to achieve its genetic growth potential in utero.
GO gene sets: Gene sets (N=5917 total) that are involved in a particular biologic process (BP), cellular component (CC), or molecular function (MF).
Hallmark gene sets: Gene sets (N=50 total) that represent stable and well-defined biological activities.
Jaccard similarity: A measure of the overlap between 2 sets. Formally, if C and D are 2 finite sets, then the Jaccard similarity between C and D is defined to be the elements in the intersection of C and D divided by the elements in the union of C and D.
Mixture-model–based clustering (*mclust* package): Algorithm for the identification of the Gaussian mixture model that best fits the data (ie, minimizes the Bayesian Information Criterion). Here, the data is modeled as having arisen from a small set of multivariate Gaussian distributions. After the optimal model of this form is identified, samples are assigned to the Gaussian distribution that they are most likely to have arisen from, and the resulting partition is referred to as a clustering of the data.
***oligo* library:** R library for preprocessing Affymetrix (Santa Clara, CA) and NimbleGen (Madison, WI) microarray data. Notably includes the robust multiarray average (RMA) method for background correction and normalization.
Pathway enrichment analysis: Refers to any method for the determination of whether a set of genes is expressed differentially between 2 sample groups.
***plot3d* function:** Function in R (included in the *rgl* package) that plots the first 3 principal components (principal component [PC] 1, 2, and 3) that are obtained from principal component analysis (PCA). These 3 components represent the most variability in the data set. Samples that plot closer together are more similar.
Preeclampsia: The onset of hypertension (systolic pressure ≥140 mm Hg and/or diastolic pressure ≥90 mm Hg) after 20 weeks gestation with proteinuria (>300 mg protein/d or ≥2+ by dipstick).
Preterm: Delivery at <34 weeks gestation.
Principal component analysis (PCA): A linear method of data reduction that converts high dimensional data (eg, gene expression data) into new independent weighted variables called "principal components" (PCs). Genes that have highly linearly correlated expression and that are responsible for the most variance in the data will contribute the most to the first principal component (PC1). Those weighted strongly in principal component 2 (PC2) are those that contribute the second greatest to the data variance and exhibit a significant linear correlation to each other, but are independent of PC1. This continues for PC3 onwards, depending on the number of samples. Once the contribution of each gene to each principal component is determined, these are used in combination with the original expression values to calculate a weighted score for each sample for each component.
Robust multiarray average (RMA): Method for converting Affymetrix (Santa Clara, CA) probe-level data to a measure of gene expression. The primary steps of the algorithm are the removal of background noise, quantile normalization, and a log-transformation.
***sigpathway* algorithm:** An algorithm for pathway enrichment analysis. Independently tests 2 different null hypotheses, corresponding to 2 different definitions of differential expression of a gene set between 2 sample groups. The first hypothesis, Q1, identifies whether the gene set is significantly differentially expressed in comparison with the global expression levels; the second hypothesis, Q2, simply evaluates whether the gene set is significantly differentially expressed between the 2 groups. In our study, Q2 was used as the main statistical test. The original method for testing for Q1 was not used but was replaced by a different heuristic that addresses the same null hypothesis (Supplementary Methods).
Small-for-gestational-age (SGA): Neonatal birthweight <10th percentile for gestational age and sex.
t-distributed stochastic neighbor embedding (t-SNE): A nonlinear method of data reduction that works by calculating distance-based similarity scores among all the samples in high-dimensional space and then randomly projecting the sample points onto a 2- or 3-dimensional plot. With each iteration, a given sample is moved closer to other samples with high similarity scores and farther from those with low similarity scores until the relationships between the points (ie, the matrix of similarity scores) in low-dimensional space reflects the relationships between the points in the original high dimensional space or the set maximum number of iterations is reached.
t-SNE plot: Visualization of t-SNE results. Unlike with PCA, the number of dimensions to be plotted (2 or 3) is preestablished and are all used to demonstrate the relationships between the points. Samples that plot closer together are more similar.
Unsupervised clustering analysis: The identification of groups of samples based solely on similarities or dissimilarities in gene expression (or histologic/proteomic/metabolomic, etc) profiles, independent of clinical diagnosis or characteristics.
***virtualArray* package:** An R library for combining microarray data from multiple studies. Removes genes that were not measured across all studies and then performs Empirical Bayes batch correction to create a final combined dataset.

SUPPLEMENTARY FIGURE

Visualization of the technical replicates by t-distributed stochastic neighbor embedding (t-SNE)

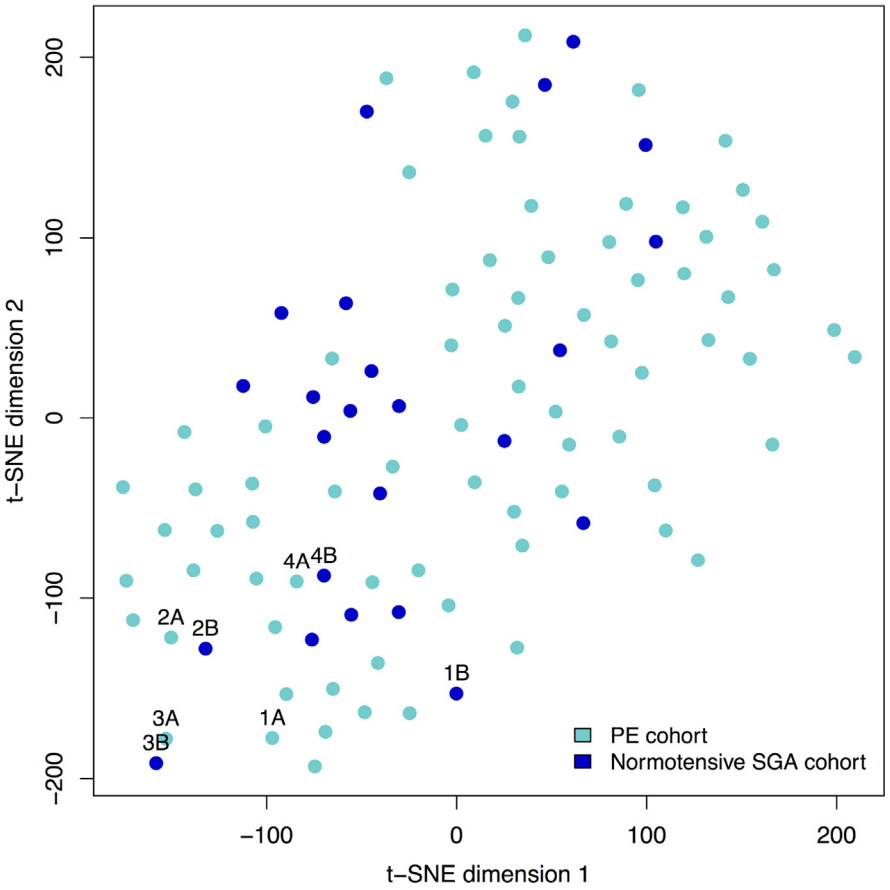

T-distributed stochastic neighbor embedding was performed on all 101 originally aggregated samples (n=97+4 technical replicates) and the top quartile of variable genes to obtain a 2-dimensional representation of the molecular similarities between placentas. As expected, the technical replicates (4 healthy control replicates from our previous preeclampsia-focused cohort [*cyan*] and the second assessment of these samples as part of our small-for-gestational-age–focused cohort [*blue*]) plotted beside each other, which indicated that batch correction was successful.

PE, preeclampsia; *SGA*, small-for-gestational-age; *t-SNE*, t-distributed stochastic neighbor embedding.

Gibbs et al. Molecular placental subtypes of normotensive FGR. Am J Obstet Gynecol 2019.